RESEARCH ARTICLE SUMMARY

CROP SCIENCE

Resetting of a tandem microRNA156 enables vegetative perennial growth in rice

Bingxin Dai†, Danfeng Lv†, Erwang Chen†, Zhoulin Gu, Dongling Guo, Yan Li, Yaoxin Zhang, Kun Liu, Ahong Wang, Qiang Zhao, Yan Zhao, Qingqing Hou, Yongchun Wang, Qi Feng, Danlin Fan, Congcong Zhou, Qilin Tian, Zixuan Wang, Jia-Wei Wang*, Bin Han*

Full article and list of author affiliations: https://doi.org/10.1126/science.adv2188

INTRODUCTION: Plants exhibit a wide variety of life history strategies. Rice (*Oryza sativa*), one of the most widely grown staple crops worldwide, is cultivated as an annual species, whereas several of its wild relatives, such as *Oryza rufipogon*, display a perennial growth habit characterized by sustained vegetative growth and repeated reproduction. During domestication, this perennial growth habit was largely lost, representing an important shift in the life history strategy of rice. However, the genetic basis responsible for this transition remains poorly understood.

RATIONALE: To address this question, we investigated the traits associated with the perennial growth habit using 446 accessions of perennial wild rice. In *O. rufipogon*, one of the key traits linked to its perennial growth habit is a grasslike plant architecture, characterized by extensive tillering, floral reversion, and vegetative propagation—a phenotype largely absent in modern cultivated rice. To delineate the genetic basis underlying this trait, we used a set of single-segment substitution lines derived from both wild and cultivated rice and identified a gene locus that harbors tandem microRNA156 genes (*MIR156BC*). Through expression pattern analysis and epigenomic profiling, we investigated how dynamic changes in miR156 abundance promote a vegetative perennial growth habit in *O. rufipogon*. Finally, we explored whether we could reproduce the vegetative perennial growth habit of *O. rufipogon* in cultivated rice by introgressing this gene locus along with loci associated with prostrate growth.

RESULTS: We identified *Endless Branches and Tillers 1* (*EBT1*) as a key gene locus controlling vegetative propagation and floral reversion in *O. rufipogon* W1943. The *EBT1* locus harbors two tandem *MIR156BC* genes and has been positively selected for. Whereas wild-type cultivars senesce after seed setting, plants carrying the *EBT1* allele from *O. rufipogon* W194 ($EBT1^{W1943}$) exhibit vigorous tiller bud outgrowth and sustained vegetative growth after flowering. Mechanistically, unlike *MIR156BC* in modern annual cultivars, *MIR156BC* expression in *O. rufipogon* can be reset in developing tiller buds after flowering. This expression pattern is associated with increased chromatin accessibility and a reduction in the repressive epigenetic marker H3K27me3 at a regulatory region of *EBT1*. The combination of *PROSTRATE GROWTH 1*, *TILLER INCLINED GROWTH 1*, and $EBT1^{W1943}$ enables annual cultivated rice to largely recapitulate the vegetative perennial growth habit of *O. rufipogon*.

CONCLUSION: We have identified *MIR156BC* as a key determinant of perenniality in rice. The distinctive epigenetic state at the *MIR156BC* locus in *O. rufipogon* facilitates its resetting after flowering, which subsequently leads to floral reversion and vegetative perennial growth. Our findings not only offer fresh insights into the genetic basis of perenniality in cereals but also pave the way for the development of sustainable perennial rice cultivars in the future. □

*Corresponding author. Email: jwwang@cemps.ac.cn (J.-W.W.); bhan@ncgr.ac.cn (B.H.)
†These authors contributed equally to this work. **Cite this article as** B. Dai *et al.*, *Science* **391**, 1239 (2026). **DOI:** 10.1126/science.adv2188

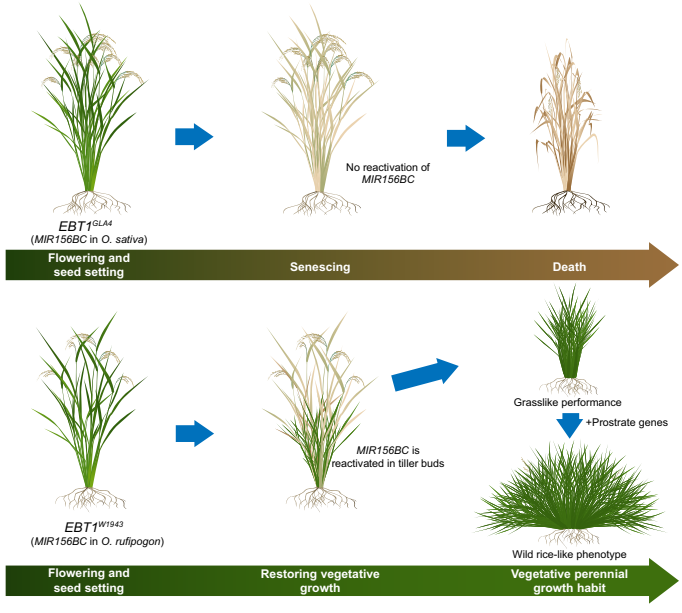

Reactivation of *MIR156BC* mediates the shift from annual to vegetative perennial growth in rice. (Top) Cultivated rice follows a determinate life cycle from flowering and seed set to senescence, without reactivation of *MIR156BC*. (Bottom) In cultivated rice carrying the wild rice *MIR156BC* allele, *MIR156BC* is reactivated in tiller buds after seed maturation, which enables continued growth and a grasslike performance characterized by floral reversion and vegetative propagation. Additional introgression of prostrate growth genes further transforms the plant into a wild-like form, supporting vegetative perennial growth.

CROP SCIENCE

Resetting of a tandem microRNA156 enables vegetative perennial growth in rice

Bingxin Dai[1]†, Danfeng Lv[1]†, Erwang Chen[1]†, Zhoulin Gu[1], Dongling Guo[1], Yan Li[1], Yaoxin Zhang[1], Kun Liu[1], Ahong Wang[1], Qiang Zhao[1], Yan Zhao[1], Qingqing Hou[1], Yongchun Wang[1], Qi Feng[1,2], Danlin Fan[1], Congcong Zhou[1], Qilin Tian[1], Zixuan Wang[1], Jia-Wei Wang[2,3,4]*, Bin Han[1]*

Annual cultivated rice was domesticated from perennial wild rice, yet the genetic mechanism of perennial growth habit remains unclear. Using introgression lines of wild and cultivated rice, we identified the *Endless Branches and Tillers* (*EBT1*) locus, comprising tandem microRNA156 genes (*MIR156BC*). This locus is responsible for floral reversion and vegetative propagation contributing to perennial growth in wild rice. The wild rice allele *EBT1*^{W1943} exhibits higher chromatin accessibility and lower levels of the repressive histone mark H3K27me3 to reset *MIR156BC* expression in tiller buds compared with the cultivated allele. Additionally, we introgressed *EBT1* and prostrate growth genes *PROG1* and *TIG1* to generate recombinant lines exhibiting a robust perennial habit. Our findings pave the way for developing sustainable perennial rice cultivars in the future.

Flowering plants are generally categorized into annual, biennial, and perennial on the basis of the length of their life cycle. However, the distinction between annuals and perennials is not absolute because these strategies are shaped by specific environmental conditions (*1*). Phylogenetic evidence suggests that annuals often evolved from perennial ancestors within specific plant lineages, but the direction of life history evolution is highly variable across taxa (*1*). For instance, cultivated rice *Oryza sativa*, domesticated over thousands of years, is an annual, whereas its wild relative *Oryza rufipogon*, which is widely considered a progenitor of cultivated rice, is a perennial (*2*–*5*). These divergent life strategies have evolved in response to domestication over relatively short evolutionary timescales, creating species with varying life history traits (*6*).

In *Arabidopsis thaliana* and *Arabis alpina*, *FLOWERING LOCUS C* (*FLC*) and its ortholog *PERPETUAL FLOWERING 1* (*PEP1*) act as floral repressors and are transcriptionally down-regulated after exposure to cold (*7*). Differential expression of three *FLC*-like genes in the vernalization pathway is crucial for the transition from polycarpic to monocarpic life histories in the *Brassicaceae* (*8*). The evolution from polycarpic perennials to biennial and annual flowering behaviors represents a continuum determined by the dosage effects of these three MADS-box genes (*9*). Consequently, research on perenniality in the *Brassicaceae* has primarily focused on vernalization and the number of flowering episodes as key aspects of perennial life strategies. In contrast to *Arabidopsis*, wild rice neither requires vernalization nor has an *FLC* ortholog, which raises a key question: What genetic mechanisms underlie perenniality in wild rice?

We investigated 446 wild rice *O. rufipogon* accessions and found that some of them exhibit strong floral reversion and vegetative propagation abilities, which are associated with clonal growth and perenniality (*10*, *11*). Using a substitution line population of wild and cultivated rice, we identified the *EBT1* locus, which consists of two microRNA156 genes arranged in tandem, as the casual gene responsible for the loss of vegetative propagation ability during domestication.

Results

Wild alleles of *EBT1* confer floral reversion and vegetative propagation ability

The wild rice *O. rufipogon* is of creeping growth and vegetative propagation, resulting in a perennial growth habit. Grasslike performance in wild rice has the following characteristics: (i) continual branch growth, (ii) sterile secondary tillers, and (iii) narrow leaves emerging from the nodes on the slender culm.

To identify the genes underlying natural variations in grasslike performance, we screened a large number of chromosome single-segment substitution lines (CSSLs) and backcross inbred lines (BILs) derived from a cross between the cultivar *O. sativa* ssp. *indica* GLA4, which exhibits a normal plant architecture, and a wild rice *O. rufipogon* accession W1943 (fig. S1, A to Q). A CSSL, G43, demonstrated the ability to undergo floral reversion and vegetative propagation after flowering (Fig. 1, A and B). Specifically, although GLA4 and G43 showed no substantial differences in tillering at the heading stage, the spikes of primary tiller of G43 matured normally, just like GLA4 (Fig. 1F and fig. S2, A and B). However, G43 produced clustered tillers with a grasslike phenotype during the late maturity stage (Fig. 1, A and B). These tillers featured elongated internodes and abnormal floral development in the secondary tillers, resulting in poor seed set. By contrast, the secondary tillers of GLA4 set seeds normally (fig. S2, C and D). At the late maturity stage, GLA4 had ~10 fertile secondary tillers, whereas G43 could produce an average of more than 70 sterile secondary tillers (Fig. 1G). Accordingly, we named the candidate gene regulating grasslike performance *Endless Branches and Tillers* (*EBT1*). Additionally, significant differences were observed in leaf width and grain number per spike between GLA4 and G43, with GLA4 having larger leaf width and a higher grain number per spike compared with G43 (Fig. 1, H and I). At 70 days after sowing, both GLA4 and G43 exhibited normal growth with no apparent differences, and secondary tillers had not yet developed (Fig. 1D). By 95 days after sowing, secondary tillers of G43 began to grow, with the second and third internodes showing development of secondary tillers, whereas the first node (counting downward from the main panicle) did not exhibit secondary tiller (Fig. 1G) growth (Fig. 1D). Meanwhile, secondary tiller growth in GLA4 was relatively slow and still in the bud stage. By 110 days after sowing, the number of secondary tillers in G43 showed a strong accelerating increase, whereas in GLA4, one primary tiller had produced only one fertile secondary tiller (Fig. 1D). The tops of the secondary tillers in G43 formed an abnormal flower composed of spathes (Fig. 1E). Additionally, G43 exhibited strong vegetative propagation ability—a small tiller separated from the mother plant can grow into a cluster of plants with dozens of tillers (fig. S2E). These clusters of plants survived in a greenhouse for at least 2 years (fig. S2E).

We observed significant morphological differences in inflorescence development between GLA4 and G43 (Fig. 1, J and O). GLA4 showed complete primary branches (Fig. 1, K to M), and the primary and secondary branch meristems developed into terminal spikelet meristems (Fig. 1N). By contrast, G43 displayed leaf primordia as small bulges on the flank of the shoot apical meristem (SAM) (Fig. 1P), and these bulges grew toward the apex and the opposite side of the SAM, forming a crescent-shaped primordium (Fig. 1Q). The primordia became hood-shaped through rapid cell division and elongation in the apical and marginal regions (Fig. 1, R to T).

The common region shared by G43 and G19 (another CSSL with grasslike phenotype) was identified on the short arm of chromosome 1 (fig. S2G). We selected G43 as the parental line for subsequent positional

[1]National Center for Gene Research, CAS Center for Excellence in Molecular Plant Sciences (CEMPS), Institute of Plant Physiology and Ecology (SIPPE), Chinese Academy of Sciences (CAS), Shanghai, China. [2]Key Laboratory of Plant Carbon Capture, CEMPS, SIPPE, CAS, Shanghai, China. [3]School of Life Science and Technology, ShanghaiTech University, Shanghai, China. [4]New Cornerstone Science Laboratory, Shanghai, China. ***Corresponding author. Email: jwwang@cemps.ac.cn (J.-W.W.); bhan@ncgr.ac.cn (B.H.)** †These authors contributed equally to this work.

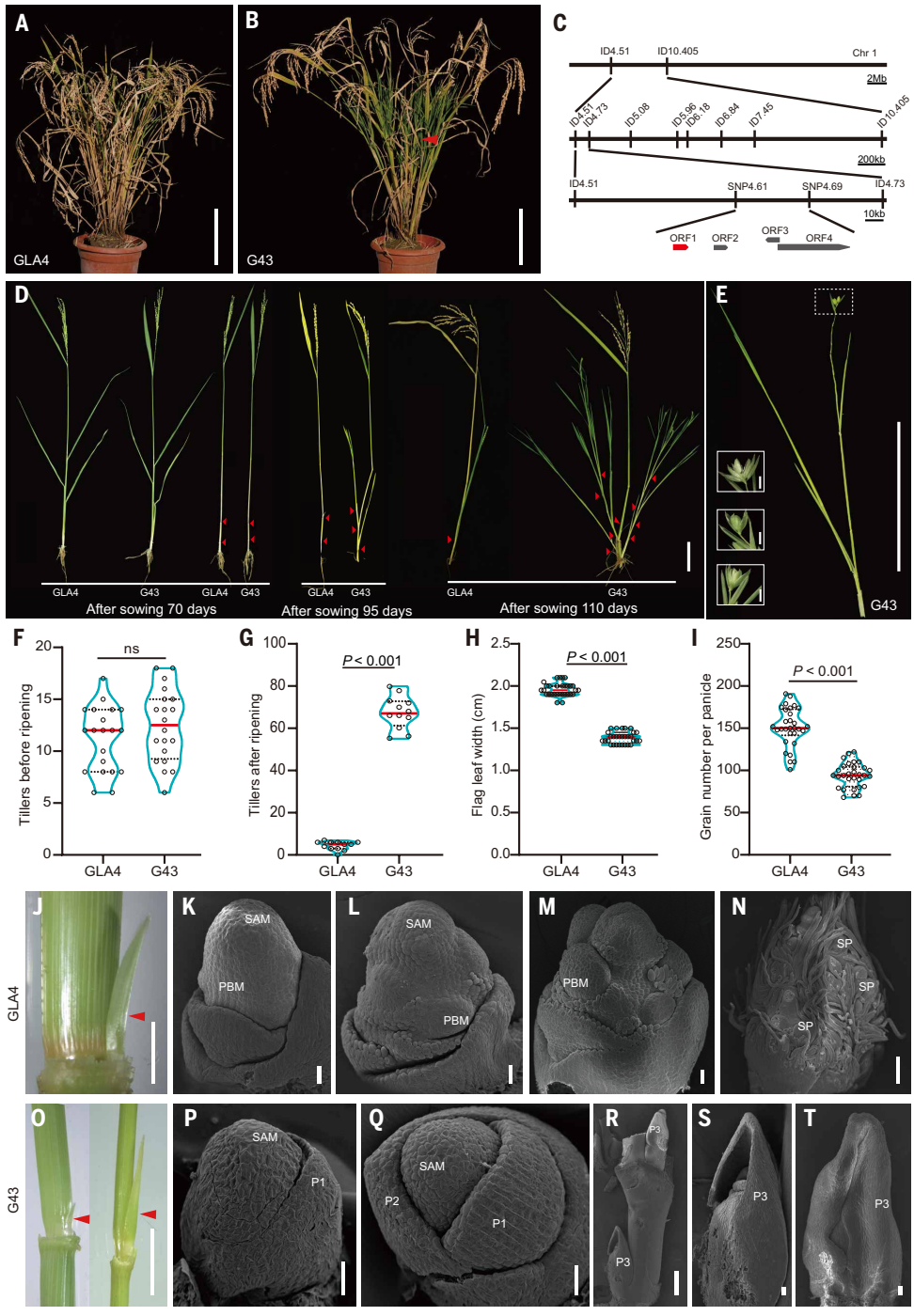

Fig. 1. Identification of *EBT1*. (**A** and **B**) Branching performance of tillers at the harvested stage of GLA4 (A) and CSSL G43 (B). The red arrowhead in (B) indicates the secondary tiller in the floral reversion state. Scale bars, 20 cm. (**C**) Map-based cloning of *EBT1*. Chr, chromosome; ORF, open reading frame. (**D**) Secondary tillers develop continuously from new buds over time in GLA4 and G43; red arrowheads indicate nodes. Scale bar, 10 cm. (**E**) Morphology of the florets at the top of the secondary tillers, which consists of multiple layers of metamorphosed leaves. Scale bars, 10 cm and 5 mm (insets). (**F** to **I**) Measurements of the number of tillers before seed ripening (F), number of tillers after seed ripening (G), flag leaf width (H), and grain number per panicle (I) in GLA4 and G43. $n = 20$ plants. Statistics by two-tailed Student's t test. ns, not significant. (**J** to **T**) Stereoscopic and scanning electron micrographs of branching axillary buds in GLA4 [(J) to (N)] and G43 [(O) to (T)] after maturity. P1, P1 primordium; P2, P2 primordium; P3, P3 primordium; PBM, primary branch meristem; SP, spikelet primordium. Scale bars, 5 mm [(J) and (O)], 20 μm [(K) to (M) and (P) to (S)], 100 μm (N), and 200 μm (T).

cloning and narrowed down *EBT1* to an ~80-kb region, which contains nine annotated genes (Fig. 1C and fig. S3D).The *EBT1* locus contained two *MIR156* genes (*MIR156BC* and *Os01g0187200*) arranged in tandem, which was highly conserved among cereals (*12*). In the maize *Corngrass1* mutant, which also contains the same tandem *MIR156* duplication, there is continual initiation of axillary branches (tillers) and leaves. This prolongs the vegetative phase, shortens internodes with adventitious roots, and results in a bushy phenotype (*13*). Additionally, overexpression of *MIR156e* or *MIR156f* results in a multitillering phenotype in rice (*14*–*16*). Therefore, the phenotypic similarities observed between *O. rufipogon*, the *Corngrass1* mutant, and rice *MIR156* overexpression lines suggest that *MIR156BC* may be the causal gene responsible for the grasslike performance in G43.

Tandem *MIR156* genes are responsible for the grasslike performance of G43

To verify whether *MIR156BC* is responsible for the grasslike performance of G43, we attempted to generate its knockout mutants. Sequence alignment revealed four nucleotide differences in *MIR156BC* between GLA4 and G43, all of which were located in the noncoding region (fig. S3E). Two mutants in the G43 background exhibited large fragment deletions in *MIR156BC*: one with a substantial deletion ($EBT1^{CR\text{-}3}$) and another with a partial deletion of *MIR156BC* ($EBT1^{CR\text{-}2}$), both resulting in a disruption of the stem-loop structure of pri-miR156bc transcripts (Fig. 2B). Compared with G43, neither $EBT1^{CR\text{-}2}$ nor $EBT1^{CR\text{-}3}$ displayed elongated internodes or developed secondary tillers (Fig. 2, C to E, G, and H). The third mutant, $EBT1^{CR\text{-}1}$, which had only a few

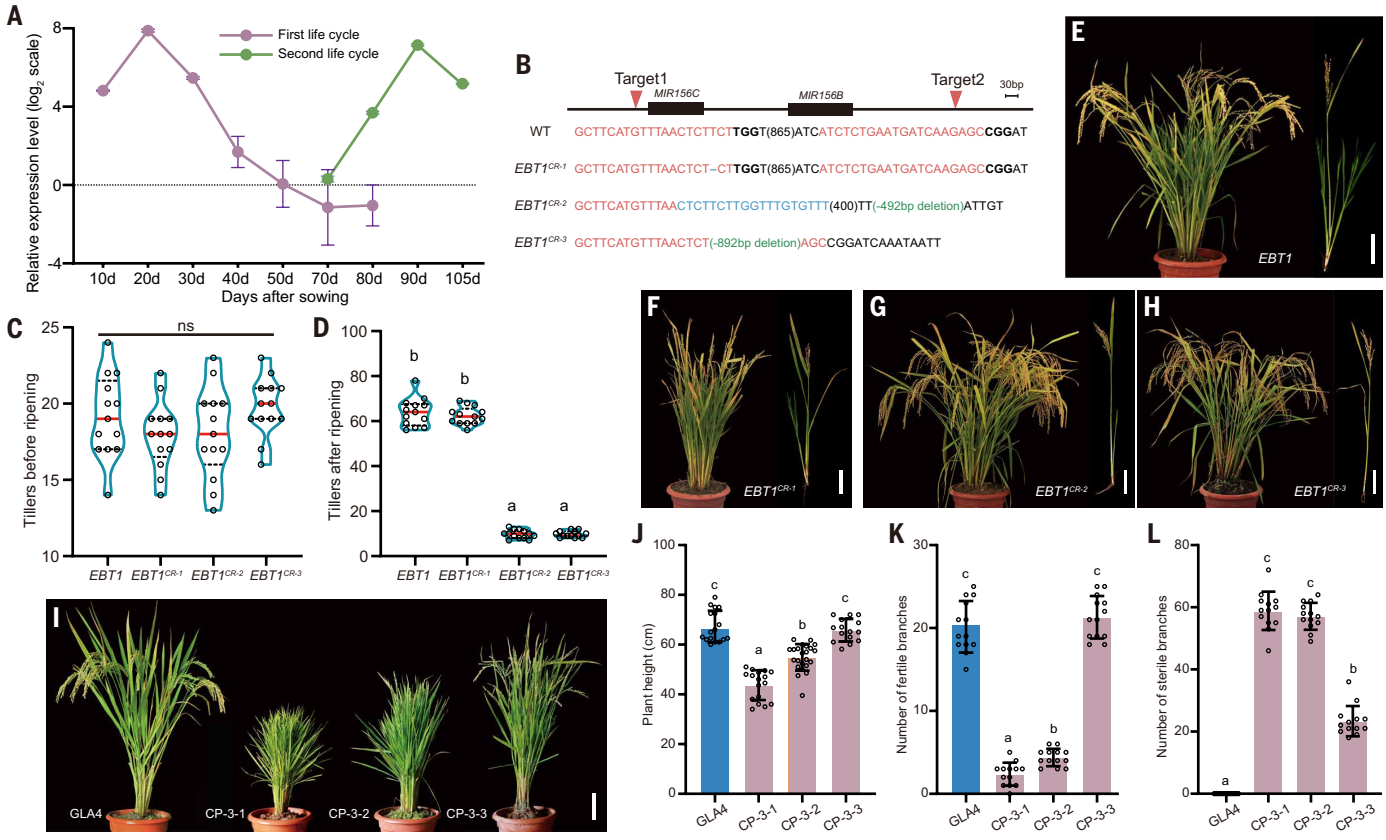

Fig. 2. *EBT1* controls branching after seed ripening. (**A**) Expression patterns of *EBT1* in leaves detected by reverse transcription quantitative polymerase chain reaction (RT-qPCR) in G43. The stage from normal seedling development to seed maturity is referred to as the first life cycle, and the stage of branch growth from nodes after maturity is called the second life cycle. Each analysis was performed with three biological replicates. Expression values are $\log_2$-transformed and shown as means ± SDs. (**B**) Diagram showing CRISPR-Cas9 editing target sites on both sides of *MIR156BC*. Two target sites are highlighted in red. WT, wild type. (**C** and **D**) Statistical analysis of tillers numbers before ripening (C) and secondary tillers numbers (D). $n = 15$ plants. a and b were measured by Tukey's honestly significant difference (HSD) test ($P < 0.05$). (**E** to **H**) Whole-plant phenotype of *EBT1* [G43 in (E)], *EBT1*$^{CR\text{-}1}$ (F), *EBT1*$^{CR\text{-}2}$ (G), and *EBT1*$^{CR\text{-}3}$ (H) at maturity. In each panel, the right side shows an isolated tiller from the plant. Scale bars, 15 cm. (**I**) Whole-plant phenotypes of complemented transgenic lines (CP-3-1, CP-3-2, and CP-3-3) and the wild-type control (GLA4). Scale bar, 10 cm. (**J** to **L**) Statistical analysis of plant height (J), tiller numbers before ripening (K), and number of secondary tillers (L) among GLA4, CP-3-1, CP-3-2, and CP-3-3. $n = 15$ plants. a, b, and c were measured by Tukey's HSD test ($P < 0.05$).

missing bases in *MIR156BC*, did not show any phenotypic differences compared with G43 (Fig. 2, B and C to F).

We also cloned three different length *EBT1* genomic fragments from G43 and introduced them into GLA4 (fig. S4A). For two of the variants, CP-1 and CP-2, 24 T_0 transgenic lines all exhibited dwarfism, multiple tillers, and sterility (fig. S4, B to G), resembling the phenotype associated with *miR156* overexpression phenotype. These lines could only be propagated asexually. For CP-3, 19 T_0 plants showed a similar phenotype to those of the CP-1 and CP-2 lines. The remaining five plants, which developed normally in the T_0 generation, were further propagated to the T_2 generation for phenotypic observations (Fig. 2I). Among these, the CP-3-3 line displayed a phenotype akin to that of G43, with no obvious differences between CP-3-3 and G43 in plant height and number of tillers before maturity, and CP-3-3 could also produce dozens of secondary tillers after flowering (Fig. 2, I and J). Although the primary tillers were not significantly different from those of GLA4, CP-3-3 produced sterile secondary tillers (Fig. 2, K and L). As a control, the 14.0-kb *EBT1* upstream fragment (CP-be) transformed into GLA4 yielded 20 T_0 lines showing wild-type tillering and fertility (fig. S4A). Taken together, these results indicate that *EBT1*, which harbors two tandem *MIR156* genes, is responsible for grasslike performance of G43.

miR156 serves as a marker gene for the juvenile-to-adult phase transition in plants, exhibiting higher expression levels in seedlings, which gradually decrease with age (*17*, *18*). We examined *EBT1* expression in G43 leaf samples at different developmental stages after sowing. *EBT1* exhibited dynamic expression changes, showing a gradual decrease in expression with age during the vegetative phase. However, after flowering, *EBT1* levels increased in newly grown leaves at day 70, coinciding with the initiation of the second life cycle (Fig. 2A). A Pro*EBT1*:GUS reporter gave similar expression results (fig. S5, A to F).

Restoration of *SPL14* or *SPL17* expression abolishes grasslike phenotype

miR156 regulates the juvenile-to-adult phase transition and flowering through its targets, *SQUAMOSA PROMOTER BINDING PROTEIN–LIKE* (*SPL*) genes (*17*, *18*). We mutated some of the *SPL* genes in GLA4, organizing them into three groups on the basis of expression patterns (fig. S5G and fig. S6). We found that *spl7 spl14 spl17* triple mutants exhibited an increase in tiller number and a decrease in plant height (fig. S7, A and B), but there were no significant changes in *spl11 spl12* or *spl2 spl4* double mutants (fig. S7G). The *spl7 spl14* double mutant had a more moderate phenotype compared with *spl7 spl14 spl17* (fig. S7A). Given that *SPL14* is a key regulator of plant architecture (*19*, *20*), we proposed that *SPL17* may also play a role in controlling plant architecture and may be involved in the floral reversion and vegetative propagation in wild rice.

We used the *EBT1* promoter to express *SPL14* or *SPL17* in G43. Compared with G43, both plants exhibited a fertile secondary tiller phenotype (fig. S7, C to F). Additionally, single-plant yield measurements showed a 30% yield recovery in these lines compared with G43 (fig. S7H). These results indicate that the increased level of *MIR156BC* after flowering in G43 leads to the formation of nonproductive tillers, which are detrimental to yield.

Polymorphisms in the *EBT1* promoter underlie variation in the grasslike phenotype

The four mutations in the stem-loop region of *MIR156BC* appear to minimally contribute to grasslike phenotype. Therefore, it is highly likely that variations in the promoter region of *MIR156BC* play a significant role in regulating its expression. We identified key single-nucleotide polymorphisms (SNPs) that may cause floral reversion and vegetative propagation after flowering. We selected 26 wild rice species with grasslike phenotype and 30 other wild rice plants lacking this phenotype for association mapping analysis. Within the 4.0-kb promoter region, 20 SNPs exhibited strong signals linked to the grasslike phenotype, with 11 SNPs showing differential patterns between GLA4 and G43, primarily located between positions −967 and −131 base pairs (bp) (fig. S8A).

We conducted whole-genome bisulfite sequencing (WGBS) on the leaves from the tillers of GLA4 and G43 at day 105. We observed differential DNA methylation levels in the *MIR156BC* promoter region between GLA4 and G43. Specifically, the DNA methylation level was higher in GLA4 than in G43, primarily occurring within a 300-bp region between transposons and *MIR156BC* (fig. S9A). These results further confirm the role of this region in the variation associated with the grasslike phenotype in rice.

A genomic region resets *MIR156BC* after flowering

We generated a series of genome-edited lines with mutations or deletions in region −967 to −131 bp of the *EBT1* promoter in G43. We analyzed 10 independent T_1 plants that harbored various mutations, including single-base mutations, small deletions, and large deletions (Fig. 3, A and C). Specifically, we assessed both effective (tillers before seed ripening) and ineffective tiller numbers (tillers after seed ripening) over a period of 2 years (Fig. 3E). Additionally, we examined *MIR156BC* expression levels in tiller axillary buds at the grain filling period (Fig. 3D). Five lines with high expression levels similar to G43 developed numerous sterile secondary tillers. Five lines with low expression levels of *MIR156BC* bore few fertile secondary tillers (Fig. 3, F to O). These results indicate that *EBT1* expression levels in axillary buds may partially determine the fate of secondary tillers in a quantitative manner.

Emerging evidence indicates that the *MIR156* loci are subject to epigenetic regulation, with the deposition of the repressive histone mark H3K27me3 at the *MIR156a/c* gene loci negatively correlating with their expression levels in *Arabidopsis* (*21*, *22*). We examined the levels of H3K27me3 and H3K4ac at the rice *EBT1* locus in GLA4 and G43. Consistent with a high level of *MIR156BC* in G43, H3K27me3 levels at *EBT1* were lower in GLA4 compared with G43 (Fig. 3B), whereas H3K4ac levels did not differ (fig. S9B). We further performed the assay for transposase-accessible chromatin with sequencing (ATAC-seq) on tiller buds at two development stages (i.e., tiller buds at the seedling stage and those at the mature stage) in both G43 and GLA4. The accessibility of a region upstream of the *MIR156BC* transcription start site (−967 to −354 bp) was correlated with its transcriptional activity. This accessible region overlaps with the DNA sequence identified by association analysis in the genome-edited lines targeting the promoter region described above (Fig. 3A and fig. S8, A and B). At the seedling stage, there was no significant difference in the degree of chromatin accessibility of *MIR156BC* between G43 and GLA4. By contrast, at the late maturity stage, *MIR156BC* became more accessible in G43 than in GLA4 (Fig. 3B). Taken together, these results imply that *MIR156BC* undergoes epigenetic reprogramming in the tiller buds after flowering in G43, subsequently leading to the resetting of its expression.

Dynamic expression patterns of *MIR156BC* in G43 and GLA4

Owing to high sequence similarity among the 11 service miR156 loci, in situ hybridization cannot effectively distinguish between different miR156 isoforms. We constructed a promoter fluorescent reporter (*ProEBT1:GFP-N7*) in which a nuclear-localized green fluorescent protein (GFP-N7) was driven by the *MIR156BC* promoter of G43. The axillary bud at the internode of GLA4 can develop into a panicle, whereas G43 has a floral reversion structure after flowering (Fig. 4A), so we observed the *MIR156BC* reporter in axillary buds. Over time, the promoter activity of *MIR156BC* gradually decreased as cell division progressed in developing buds. In regions of active cell division, the *MIR156BC* promoter signal was strong, whereas in differentiated areas, the promoter activity was very low, with almost no detectable fluorescence signal.

MIR156BC was transcribed during the seedling stage, and the promoter activity significantly reduced as the plant aged (Fig. 4, B and C). The GFP-N7 signals progressively increased after 99 days after sowing in the second generation of newly formed axillary buds, with signal intensity even surpassing that in the seedling stage (Fig. 4C). By contrast, transgenic lines of *MIR156BC* reporter driven by the GLA4 promoter showed weak signals in secondary tillers growing alongside the main tiller (Fig. 4D and fig. S9C). In *Arabidopsis*, *MIR156A–C* (*MIR156A*, *-B*, and *-C*) are de novo activated during sexual reproduction and embryogenesis (*23*). Alongside our data, this suggests that the *MIR156BC* locus undergoes distinct reprogramming events, with a stronger reactivation observed in the tiller bud after flowering.

EBT1 was a target of selection during rice domestication

Domestication leads to a reduction of genetic diversity across the genome or in specific regions, which means that favorable alleles for important traits become enriched (*24*). We analyzed the nucleotide diversity (π) and fixation index (F_{ST}) of *EBT1* and its flanking region using a genomic dataset comprising 870 rice accessions. These included 501 diverse *O. rufipogon* accessions from Asia and Oceania, spanning the native geographic range of the species for natural growth under pot-grown conditions, and 369 cultivars. These results suggest that, in agreement with previous finding (*12*), *EBT1* may have been positively selected during rice domestication to optimize yield-related architecture. We observed that the genetic diversity decreased within the *EBT1* gene and its promoter region in cultivated rice compared with wild rice (average $\pi = 0.00601$ in wild rice; average $\pi = 0.0026$ in cultivated rice) (Fig. 4E and fig. S8C).

We further identified 15 major haplotypes in the promoter sequence of *EBT1* by using 117 wild rice, 47 *Oryza nivara*, 51 landraces, 100 *japonica*, 224 *indica*, and 16 *aus*. Hap4 and Hap5 were predominantly found in *O. rufipogon*, which tends to display perennial growth, whereas Hap1, Hap2, and Hap3 were primarily associated with annual *O. nivara*, *japonica*, and *indica* accessions (Fig. 4F and fig. S8B).

Although the grasslike phenotype can prolong the lifespan of rice and promote vigorous vegetative growth, it produces fewer seeds on the main tillers compared with cultivated rice (Fig. 1I), thereby substantially reducing grain yield. Therefore, the *EBT1* allele that drives the transition from a grasslike form to a more productive architecture with numerous effective tillers represents a domestication locus positioned at the top of a large gene regulatory network.

Introgression of *O. rufipogon* alleles to generate asexual perennial growth in an annual cultivar

O. rufipogon accessions (W156, W234, W404, and W412) showed vegetative propagation traits, resulting in a perennial growth habit (fig. S10, A to H). After flowering, the axillary buds on the secondary tiller nodes in *O. rufipogon* were leaf primordia rather than spikelet primordia (fig. S10, I to L), which indicates that these buds remained in the vegetative stage. This suggests that, after reproductive growth, the apical meristem of *O. rufipogon* can revert to vegetative growth through secondary tillers, thereby initiating a cycle of vegetative propagation. These observations

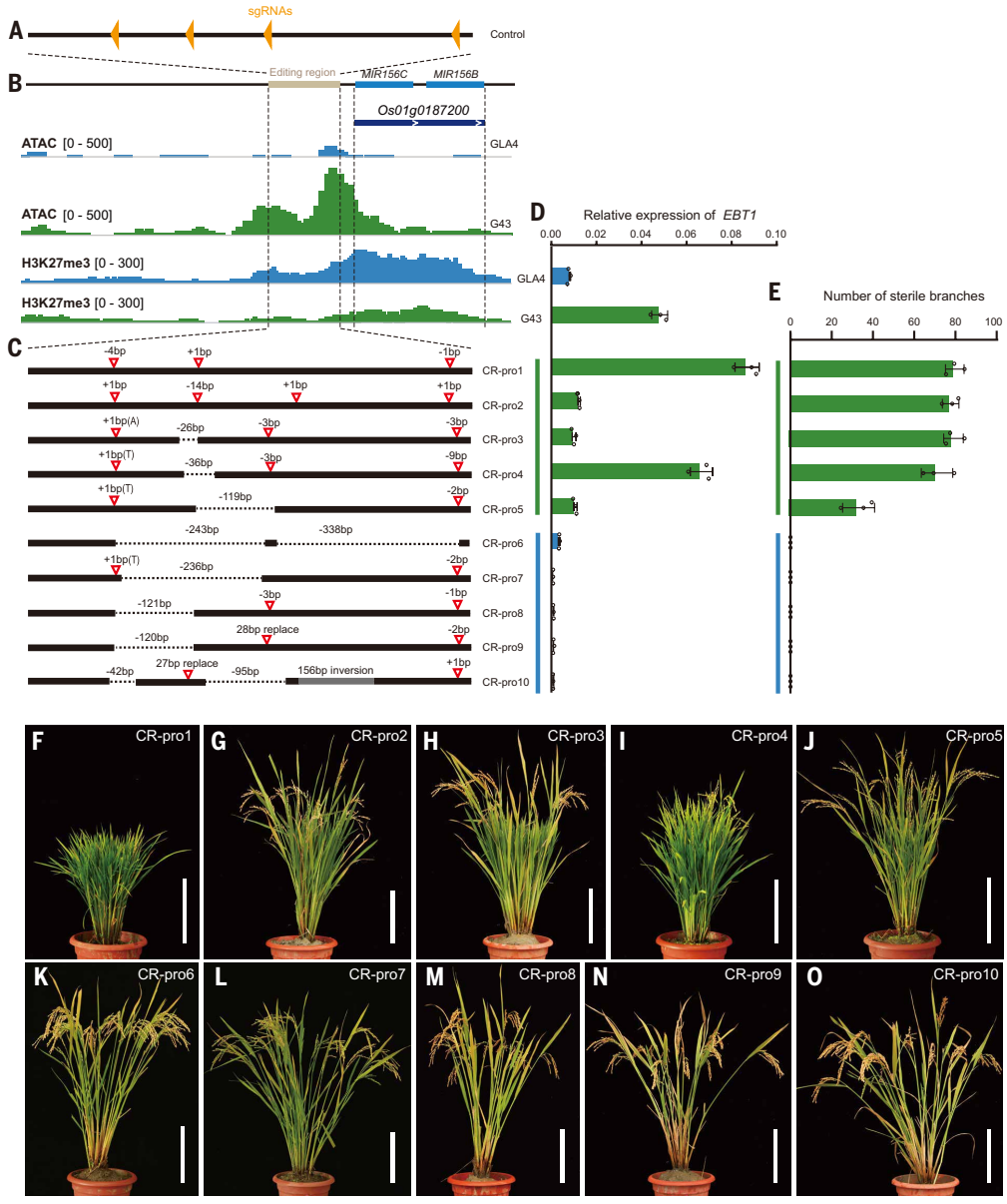

Fig. 3. A diverse collection of CRISPR-Cas9–engineered *EBT1* promoter alleles reveals complex relationships between promoter mutations and branching variation. (**A**) An expanded collection of 10 *EBT1* promoter alleles was generated using a CRISPR-Cas9 genetic drive system. CRISPR-Cas9 transgenic plants were generated by transforming a construct carrying four guide RNAs (gRNAs) targeting the *EBT1* promoter, indicated by orange arrowheads. (**B**) ATAC-seq and H3K27me3 cleavage under targets and tagmentation (Cut&Tag) profiles for the *EBT1* locus in GLA4 and G43. (**C**) Schematic representation of 10 CRISPR-Cas9–engineered EBT1pro alleles. Large deletions and inversions are represented by black dashed lines and gray boxes, respectively. Small insertions and deletions are indicated by numbers and letters. (**D**) Relative expression levels of *EBT1* in different CR-promoter lines corresponding to (C). Each analysis was performed with three biological replicates. Data are shown as means ± SDs. (**E**) Statistics of secondary tiller number in transgenic plants corresponding to the genotypes in (C). (**F** to **O**) Phenotypes of representative promoter-edited plant lines. Scale bars, 10 cm.

highlight the potential for manipulating rice growth to replicate wild rice traits, which could facilitate the development of varieties capable of perennial reproduction.

Building on this, we attempted to combine the prostrate growth gene *PROG1* (*25*, *26*), *TILLER INCLINED GROWTH 1* (*TIG1*) (*27*), and *EBT1* through hybridization to artificially create wild-like rice. In the BIL population, we selected BIL85, BIL138, BIL148, BIL250, and BIL271 (fig. S1, B, E, G, K, and O), all of which carry the *EBT1* and *Tiller Angle Control 1* (*TAC1*) gene, and crossed them with *TIG1+PROG1* plants (14W61) carrying *PROG1* and *TIG1* (fig. S11A) (*27*). After five generations of selfing, some offspring exhibited more pronounced grasslike phenotypes, which originated from specific lineages, and we named these lineages wild-like rice. Genotypic analysis revealed the presence of *PROG1*, *TIG1*, and *EBT1* in all selected lines (fig. S11, B and C). These lines not only exhibited larger tiller angles, forming a prostrate growth habit that covers a large area, but also displayed abnormal secondary branching (fig. S11, C and D). Some lateral branches grew horizontally and rooted at the nodes, with the rooted secondary shoots capable of regenerating into new seedlings. When a tiller from these plants was removed and cultured under suitable conditions, it could regenerate into a new plant, with normal flowers and seed set. After maturing, they continued to produce secondary tillers (fig. S11C). The wild-like rice plants could survive for at least 2 years in a tropical area (Hainan, southern island in China), thus achieving a perennial-like life cycle (fig. S11C).

In its natural state, wild rice has superior asexual reproduction compared with cultivated rice, not only because of its prostrate growth habit that enables the development of roots at multiple nodes, but also because it can expand its growing space through aboveground runners (fig. S12). We further examined root morphology and observed that both W1943 and wild-like rice plants developed crown tiller buds (basal-positioned adventitious shoots), albeit with distinct architectures. In W1943, the tiller buds were tightly clustered around the stem base, whereas wild-like rice plants exhibited elongated internodes with spatially dispersed buds (fig. S13, A to E). As older tillers senesce, new crown-derived buds regenerate continuously, which suggests another mechanism underlying perenniality in wild rice.

Discussion

Our results reveal that the vegetative perennial growth habit in *O. rufipogon* is primarily governed by the resetting of *MIR156BC* after

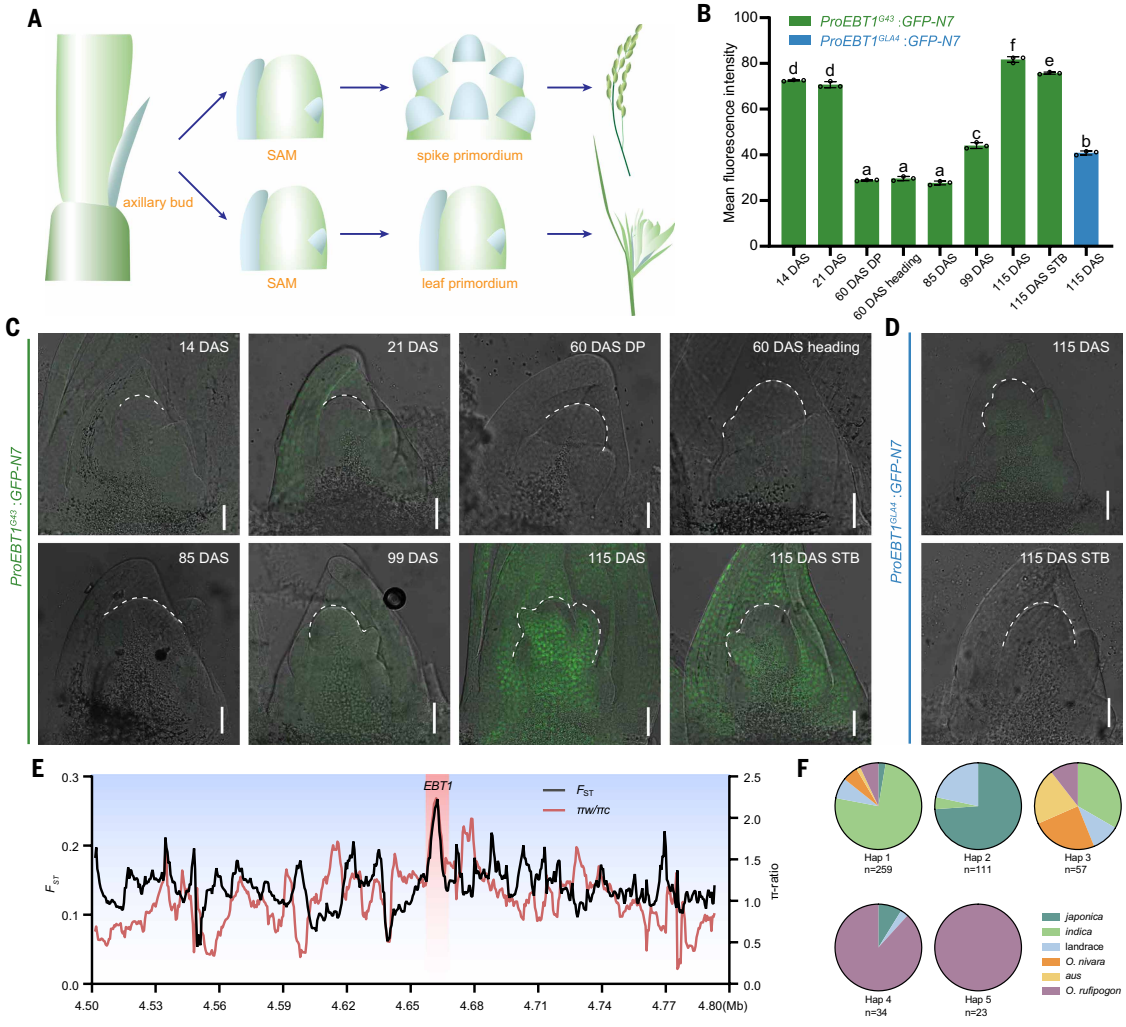

Fig. 4. Developmental trajectory of axillary buds manipulated by *EBT1* and natural variations of *EBT1*. (**A**) Schematic diagram of the developmental pattern of axillary buds at nodes in GLA4 and G43 at maturity. In GLA4, they can develop normally into spikes, whereas in G43, they develop into abnormal leaves. (**B**) Fluorescence intensity distribution at each developmental stage. Each stage includes three biological replicates. Data are presented as means ± SDs. DAS, days after sowing; DP, developmental panicles stage; heading, heading stages; STB, secondary tillers bud. Green indicates *ProEBT1^{G43}:GFP-N7* in G43, and blue indicates *ProEBT1^{GLA4}:GFP-N7* in G43. a, b, c, d, e, and f were measured by Tukey's HSD test ($P < 0.05$). (**C**) Snapshots of the live imaging of the fluorescent reporter of G43 promoter (*ProEBT1^{G43}:GFP-N7*) during the initiation of axillary buds in the main tiller. Scale bars, 50 μm. (**D**) Snapshots of the live imaging of the fluorescent reporter of GLA4 promoter (*ProEBT1^{GLA4}:GFP-N7*) during the initiation of axillary buds in the main tiller at 115 DAS. Scale bars, 50 μm. (**E**) Nucleotide diversity ratio ($\pi w/\pi c$) and fixation index (F_{ST}) between wild and cultivated rice across a region of chromosome 1. The *EBT1* locus is shaded in red. (**F**) Haplotype distribution of *EBT1* in different subspecies.

flowering (Fig. 5). This, in combination with prostrate genes, enables a grasslike growth behavior, similar to that of wild rice (fig. S12). Although these wild-like rice plants showed some perenniality traits, isolated secondary tillers of near-isogenic lines could not flower and produce seeds normally. Instead, they remained in the vegetative growth stage for at least 2 years under suitable conditions. This shows that other loci are needed to fully restore the perenniality in these plants. During phenotypic screening, we identified rare landraces lines exhibiting grasslike morphology (fig. S14). One trait that we observed is the ability of a fallen branch to produce new roots in G43, establishing a genetically identical plant. This characteristic may be specific to certain wild rice populations in particular regions, where it evolved as a strong regenerative mechanism to adapt to local environmental conditions, enabling asexual reproduction and ensuring the continuity of the population.

Collinearity analysis across the *Gramineae* revealed that the tandem organization of *MIR156BC* is evolutionarily conserved (fig. S15). Among these, wheat, barley, and bamboo each harbor three tandem copies. We speculate that the tandem configuration of *MIR156BC* facilitates precise reactivation and contributes to the multibranching behavior associated with perenniality.

In contrast to *O. rufipogon*, another wild rice species, *Oryza longistaminata*, survives cold winters through underground rhizomes and regrows in spring. Similarly, perennial maize and sorghum exhibit comparable traits (*28*–*31*). Introgression of *O. longistaminata* loci that control rhizome development into elite *O. sativa* lines has transformed major annual crops into perennials (*32*). Although *O. rufipogon* maintains perenniality without developing rhizomes, our study provides fresh insights into the nonrhizomatous perennial growth strategy of this key wild progenitor species.

Perenniality and annuality should be considered syndromes composed of many other interacting traits, such as leaf and root anatomy, resource use efficiency, and regulation of source-sink dynamics (*33*). Fully converting modern rice into a true perennial crop will require identifying these additional components and reconstructing the coordinated genetic network underlying perennial growth.

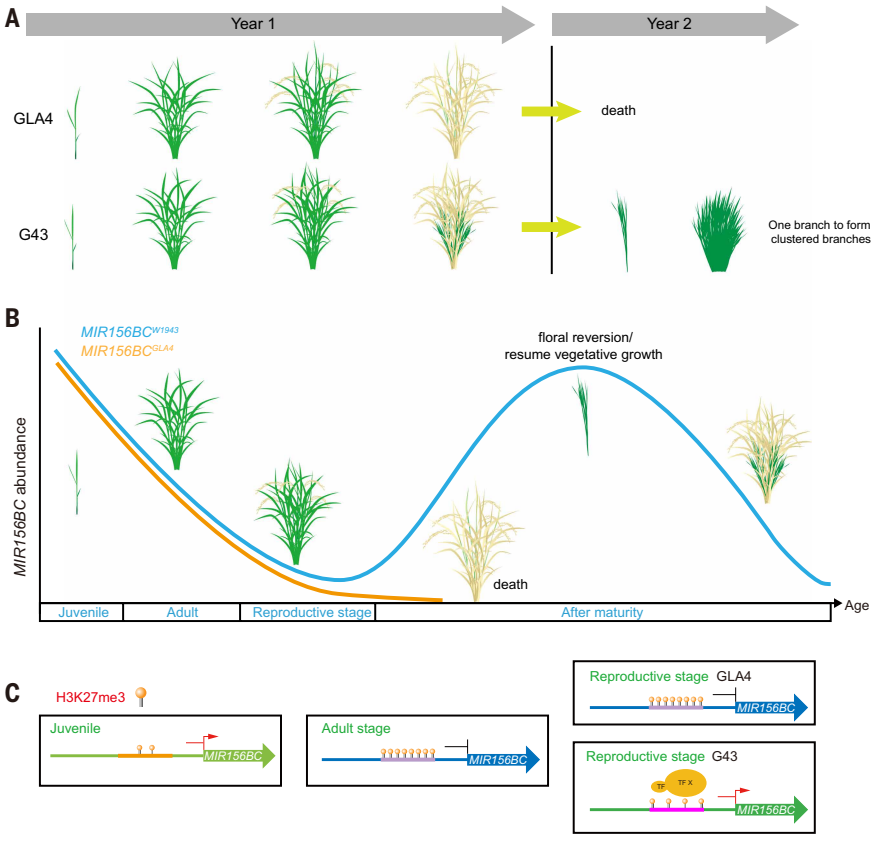

Fig. 5. Proposed model for the determination of life history–associated plant architecture. (**A**) Schematic diagram of plant types at different life stages in GLA4 and G43. Year 1 depicts growth from seedling to maturity. The right panel shows the growth state in year 2 of a branch separated from the parent plant in year 1. (**B**) Model illustrating the resetting of juvenility and MIR156BC expression during each developmental stage. *MIR156BC* expression in both GLA4 and G43 progressively decreases during vegetative development. However, *MIR156BC* expression is reset at maturity in G43, showing a high expression level. (**C**) Proposed dynamic epigenetic status at the *MIR156BC* locus. At maturity, GLA4 and G43 exhibit distinct chromatin regulatory states, with GLA4 showing enrichment of the repressive histone mark H3K27me3, whereas G43 displays reduced H3K27me3 deposition.

REFERENCES AND NOTES

1. J. Friedman, *Annu. Rev. Ecol. Evol. Syst.* **51**, 461–481 (2020).
2. M. Sweeney, S. McCouch, *Ann. Bot.* **100**, 951–957 (2007).
3. R. S. Meyer, M. D. Purugganan, *Nat. Rev. Genet.* **14**, 840–852 (2013).
4. K. M. Olsen, J. F. Wendel, *Annu. Rev. Plant Biol.* **64**, 47–70 (2013).
5. X. Huang *et al.*, *Nature* **490**, 497–501 (2012).
6. B. Zhao, J. W. Wang, *Mol. Plant* **17**, 141–157 (2024).
7. R. Wang *et al.*, *Nature* **459**, 423–427 (2009).
8. S. Bergonzi *et al.*, *Science* **340**, 1094–1097 (2013).
9. D. Zhai *et al.*, *Cell* **187**, 3319–3337.e18 (2024).
10. S. Munné-Bosch, *Plant Physiol.* **166**, 720–725 (2014).
11. W. E. Van Drunen, B. C. Husband, *New Phytol.* **224**, 1266–1277 (2019).
12. S. Wang *et al.*, *FEBS Lett.* **581**, 4789–4793 (2007).
13. G. Chuck, A. M. Cigan, K. Saeteurn, S. Hake, *Nat. Genet.* **39**, 544–549 (2007).
14. Z. Chen, X. Gao, J. Zhang, *Plant Cell Rep.* **34**, 767–781 (2015).
15. Q. Liu *et al.*, *J. Integr. Plant Biol.* **57**, 819–829 (2015).
16. Z. Dai *et al.*, *J. Exp. Bot.* **69**, 5117–5130 (2018).
17. G. Wu *et al.*, *Cell* **138**, 750–759 (2009).
18. J. W. Wang, B. Czech, D. Weigel, *Cell* **138**, 738–749 (2009).
19. Y. Jiao *et al.*, *Nat. Genet.* **42**, 541–544 (2010).
20. K. Miura *et al.*, *Nat. Genet.* **42**, 545–549 (2010).
21. Y. J. Cheng *et al.*, *Proc. Natl. Acad. Sci. U.S.A.* **118**, e2115667118 (2021).
22. M. Xu, T. Hu, M. R. Smith, R. S. Poethig, *Plant Cell* **28**, 28–41 (2016).
23. J. Gao *et al.*, *Nat. Plants* **8**, 257–268 (2022).
24. J. F. Doebley, B. S. Gaut, B. D. Smith, *Cell* **127**, 1309–1321 (2006).
25. J. Jin *et al.*, *Nat. Genet.* **40**, 1365–1369 (2008).
26. L. Tan *et al.*, *Nat. Genet.* **40**, 1360–1364 (2008).
27. W. Zhang *et al.*, *Mol. Plant* **12**, 1075–1089 (2019).
28. L. Guo, M. Plunkert, X. Luo, Z. Liu, *Curr. Opin. Plant Biol.* **59**, 101970 (2021).
29. F. Y. Hu *et al.*, *Proc. Natl. Acad. Sci. U.S.A.* **100**, 4050–4054 (2003).
30. A. H. Paterson, K. F. Schertz, Y. R. Lin, S. C. Liu, Y. L. Chang, *Proc. Natl. Acad. Sci. U.S.A.* **92**, 6127–6131 (1995).
31. A. Westerbergh, J. Doebley, *Theor. Appl. Genet.* **109**, 1544–1553 (2004).
32. S. L. Zhang *et al.*, *Nat. Sustain.* **6**, 28–38 (2023).
33. M. R. Lundgren, D. L. Des Marais, *Curr. Biol.* **30**, R180–R189 (2020).

ACKNOWLEDGMENTS

We thank Y. Mai for technical support in fluorescence-activated cell sorting (FACS) using a SONY MA900 Flow Cytometer (CAS Center for Excellence in Molecular Plant Sciences), Z. Zhang for scanning electron microscopy observation, and W. Cai (CAS Center for Excellence in Molecular Plant Sciences) for confocal microscopy observation support. We thank Y.-G. Liu (South China Agricultural University) for providing the CRISPR-Cas9 vector. We thank C. Sun (China Agricultural University) for providing the *prog1* and *tig* seeds. We thank H.-X. Lin (CAS Center for Excellence in Molecular Plant Sciences), Y. Qi (Tsinghua University), and X. Huang (Shanghai Normal University) for discussions. **Funding:** This work was supported by grants from the National Natural Science Foundation of China (32388201 to B.H. and J.-W.W.), the Ministry of Agriculture and Rural Affairs (2022YFF1003301 to B.H.), the Chinese Academy of Sciences (XDB27010301 to B.H.), the Strategic Priority Research Program of the Chinese Academy of Sciences (XDB0630200 to J.-W.W. and Q.F.), and the Science and Technology Commission of Shanghai Municipality (24N12800300). **Author contributions:** B.H., B.D., D.L., E.C., and J.-W.W. designed the study and wrote the manuscript. B.D., D.L., E.C., K.L., A.W., Q.H., D.F., C.Z., Y.L., Q.T., and Z.W. performed the experiments, and Y.W. was responsible for material planting and management. Z.G., D.G., Y.Zhao, Y.Zhan., Q.Z., Q.F., J.-W.W., and B.H. analyzed the data. **Competing interests:** B.H., B.D., E.C., K.L., Z.G., and D.L. are inventors on a granted patent in China related to this work (no. ZL202011545246.9). The other authors declare that they have no competing interests. **Data, code, and materials availability:** All data supporting the findings of this work are available within the paper and its supplementary materials. All raw sequencing data generated in this study have been deposited in the European Nucleotide Archive (ENA) under the BioProject accession no. PRJEB107304, including CUT&Tag (ERX15645892 to ERX15645907), ATAC-seq (ERX15645870 to ERX15645873 and ERX15645880 to ERX15645883), and WGBS (ERX15645311 to ERX15645312). ATAC-seq differential accessibility analyses are available at Figshare (https://figshare.com/s/5182895b6cf29d975072). No restrictions are placed on materials, such as material transfer agreements. The described rice materials can be obtained from B.H.

SUPPLEMENTARY MATERIALS

science.org/doi/10.1126/science.adv2188
Materials and Methods; Figs. S1 to S15; References (*34*–*54*); MDAR Reproducibility Checklist; Data S1 to S4

Submitted 10 December 2024; resubmitted 26 November 2025; accepted 6 February 2026
10.1126/science.adv2188

Resetting of a tandem microRNA156 enables vegetative perennial growth in rice

Bingxin Dai, Danfeng Lv, Erwang Chen, Zhoulin Gu, Dongling Guo, Yan Li, Yaoxin Zhang, Kun Liu, Ahong Wang, Qiang Zhao, Yan Zhao, Qingqing Hou, Yongchun Wang, Qi Feng, Danlin Fan, Congcong Zhou, Qilin Tian, Zixuan Wang, Jia-Wei Wang, and Bin Han

Science **391** (6791), . DOI: 10.1126/science.adv2188

Editor's summary

Most grain crops die after completing one life cycle, meaning that new plants must be sown each year. However, some wild relatives of rice are perennial and can live through multiple yearly cycles. Dai *et al*. identified a locus coding for a duplicated microRNA with expression that is regulated by DNA methylation status. Some alleles of this locus confer the ability to propagate rice vegetatively. By generating rice lines harboring this microRNA as well as genes for other perennial traits, the authors developed rice that could grow for more than a year. Although alleles of additional loci will be needed to make fully fertile perennial rice plants, this work provides insight into perennial traits in rice and is a step forward in genetic engineering efforts. —Madeleine Seale